An exploratory analysis of phosphorus transformations in tropical soils using structural equation modeling

A. C. Gama-Rodrigues · M. V. S. Sales ·
P. S. D. Silva · N. B. Comerford · W. P. Cropper ·
E. F. Gama-Rodrigues

Abstract In the tropics, highly weathered soils with high phosphorus (P) fixation capacities predominate, reducing the P availability to plants. For this reason, understanding the cycle of P in the soil is important to develop management strategies that increase P availability to plants, especially in low-input production systems. The aim of this study was to apply structural equation modeling with latent variables, at an exploratory level, to test hypothetical models of the P cycle using data from the Hedley extraction method. Specifically, we evaluated interactions between the pools of P, and identified which pools act as a sink or source of P in unfertilized soils. The models of the P cycle for the tested soil were able to distinguish between the direct and indirect effects of labile and stable P on the available P pool. This approach led to a proposed distinction of functional P pools in the soil, and identifying the processes of P transformation in the soil between the pools based on a source–sink relationship. Based on these analyses, the organic pool consists of the bicarbonate organic phosphate (Po), hydroxide Po, and sonic Po fractions. The bicarbonate inorganic phosphate (Pi) and hydroxide Pi fractions formed the inorganic pool. The hydrochloride (HCl) P_{hot} and residual P fractions formed the occluded pool, the HCl Pi fraction formed the primary mineral pool, and the resin Pi fraction constituted the most available P pool. Organic P pool was the major source to the available P pool.

A. C. Gama-Rodrigues (✉) · M. V. S. Sales ·
E. F. Gama-Rodrigues
Soil Laboratory, North Fluminense State University Darcy
Ribeiro, UENF/CCTA/LSOL, Av. Alberto Lamego 2000,
Campos dos Goytacazes, RJ CEP 28013-602, Brazil
e-mail: tonygama@uenf.br

P. S. D. Silva
Mathematics Laboratory, North Fluminense State
University Darcy Ribeiro, Campos dos Goytacazes,
RJ CEP 28013-602, Brazil

N. B. Comerford
North Florida Research and Education Center, University
of Florida, Quincy, FL 32351-5677, USA

W. P. Cropper
School of Forest Resources and Conservation, University
of Florida, Gainesville, FL 32611-0410, USA

Introduction

Phosphorus (P) deficiency is the major nutritional limitation for agricultural soils in the tropics (Grierson et al. 2004). In this context, understanding the soil P cycle is necessary to establish management efficient strategies to increase plant P availability, especially in low-input production systems. The P cycle can be divided into biological and geochemical processes (Smeck 1985; Frossard et al. 2000) that regulate the

availability of soil P (Cross and Schlesinger 1995). The method chosen for evaluating soil P pools greatly influences estimates of soil P availability. The Hedley method of sequential extraction or fractionation of P (Hedley et al. 1982) enables characterization of the different fractions of inorganic and organic P obtained based on solubility of inorganic and organic P in sequential extracting solutions based on changes different pH and extracting strength. Resin inorganic phosphate (Pi) represents an index of exchangeable P that any plant would have access to simply by removing inorganic P from the soil solution by uptake (Sato and Comerford 2006) Bicarbonate Pi and bicarbonate organic phosphate (Po) fractions index P that can be released by ligand exchange with the bicarbonate ion (Sato and Comerford 2006). Hydroxide Pi, hydroxide Po, sonic Pi, sonic Po, hydrochloride (HCl) Pi, and residual P fractions are index P forms that are much more difficult to move into the soil solution P (Cross and Schlesinger 1995).

In tropical soils, especially those that are highly weathered and clayey, the fixation capacity of P is high, reducing P availability to plants. Thus, the soil with strong buffering capacity competes with the plants for the added P, and the soil becomes a sink. In these unfertilized soils, the availability of P is highly dependent on the mechanisms that the plant roots use for accessing the range of soil P sources, both organic and inorganic. The Hedley P fractionation is an effective method for contrasting soil P forms between and among different soils and soil treatments. Fractionation of soil P alone does not permit evaluation of interactions between P fractions. Path analysis with structural equations has been used to study the magnitude of interactions between the different P fractions in temperate soils (Tiessen et al. 1984; Zheng et al. 2002). This modeling method permits the decomposition of the correlations among the observed variables into direct and indirect effects in a model where the regressions of the relationships between the variables can be simultaneously evaluated (Malaeb et al. 2000; Arhonditsis et al. 2006; Prober and Wiehl 2011). In addition, an essential characteristic of structural equation modeling (SEM) is the ability to include latent variables (not measured) together with the measurable variables in hypothetical models. The latent variables are used in the models to represent potential underlying causes, while the measurable variables serve as indicators of the effects or manifestations of the latent factors (Grace and Bollen

2008). One of the advantages of SEM is its ability to rank the descriptive ability of different models, thus enabling comparisons between the models (Mitchell 1992).

Beck and Sanchez (1994) also used path models (observed variable models) to analyze the transformations between P fractions in a tropical Ultisol. But as they did not use structural models (latent variable models) to evaluate the different P pools as latent hypotheses with multi-indicators (P fractions). Significant uncertainties remain and pathways of P transformations in tropical soils worldwide remain poorly understood. Accordingly, the present study aimed to use the method of SEM with latent variables, at the exploratory level, to evaluate hypothetical models of the P cycle and to determine the interactions among the pools of P and to identify which pools act as a P sink or source in unfertilized tropical soils. We evaluated three models in this study. Firstly, we formulated an a priori basic structural model based on our knowledge of soil P dynamics relationships among five latent variables (P pools), described by multiple indicator variables (P fractions): we expected a direct effect of organic pool, inorganic pool, occluded pool and primary mineral pool on available pool (Fig. 1). Secondly, the basic model was split into two sub-models to assess changing from a multi-indicator to single-indicator model.

Materials and methods

The soil P data were collected from the literature (see Appendix Table 7) and were restricted to studies that used the sequential fractionation technique developed by Hedley et al. (1982) and modified by Tiessen and Moir (1993). The fractions of P used were resin Pi, bicarbonate P (Pi and Po), hydroxide P (Pi and Po), sonic P (Pi and Po), HCl Pi, HCl P_{hot}, and residual P. The soil properties used in the correlations with the P fractions were pH, clay content, organic carbon (C), total nitrogen (N), iron oxides (Fe_{ox}), and aluminum oxides (Al_{ox}). The data set ($N = 81$) covers a wide range of unfertilized soil types under different land use systems in tropical regions.

Factor and path analysis

Initially, the relations between the P fractions and various soil properties (pH, clay, organic C, total N,

Fig. 1 The hypothesized structural model for the soil P cycle
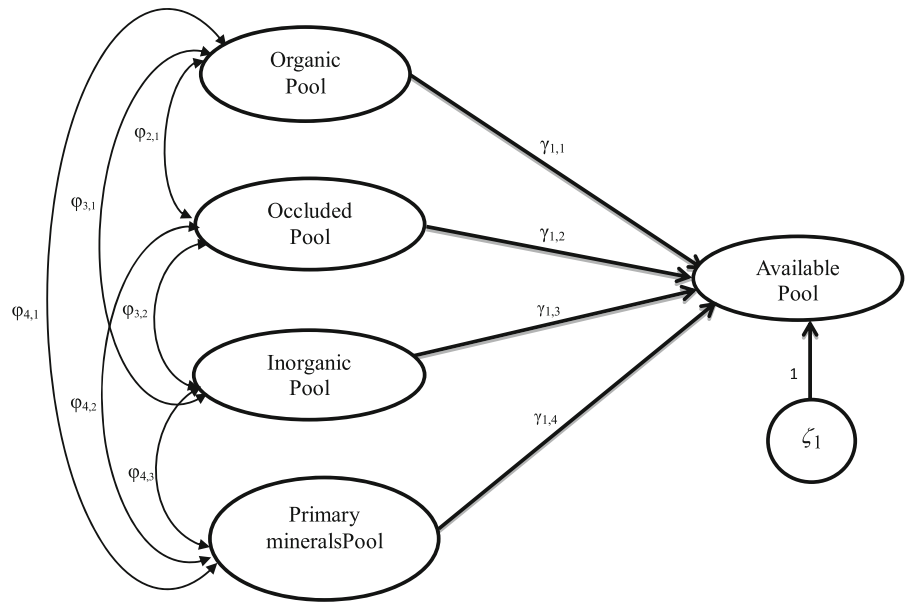
Fe$_{ox}$, and Al$_{ox}$) were determined using Pearson correlation coefficients and multiple regression analyses. We made the assumption that the correlation structure observed from the literature data is the same that we would obtain from a single random sample. We used correlation analysis to determine the intensity ratio of all of the P fractions, while the backward multiple regression analysis was used with the resin Pi fraction as the dependent variable and the other P fractions as independent variables. The P fractions (independent variable) in the soil that did not contribute significantly to the estimation of the resin Pi fraction at $P \leq 0.05$ were eliminated using stepwise regression. The model fit was measured by the determination coefficient (R^2) and by the significance of the regression and β coefficients of the direct effect of the independent variables (predictors).

The path analysis was conducted according to Williams et al. (1990) and performed in two stages: the first stage included all of the P fractions except the sonic Pi fraction (eliminated by the test of multicollinearity; data not shown), and the second stage encompassed the P fractions selected only by backward multiple regression. In the path analysis, each normal equation represents a decomposition of the correlation coefficient into direct (path coefficient) and indirect effects between the resin Pi fraction (dependent variable) and the other P fractions (independent variables). The path analysis results were

determined using the following equations (Williams et al. 1990):

$$r_{19} = \boldsymbol{P_{19}} + r_{12}P_{29} + r_{13}P_{39} + r_{14}P_{49} + r_{15}P_{59} + r_{16}P_{69} + r_{17}P_{79} + r_{18}P_{89} \tag{1}$$

$$r_{29} = r_{12}P_{19} + \boldsymbol{P_{29}} + r_{23}P_{39} + r_{24}P_{49} + r_{25}P_{59} + r_{26}P_{69} + r_{27}P_{79} + r_{28}P_{89} \tag{2}$$

$$r_{39} = r_{13}P_{19} + r_{23}P_{29} + \boldsymbol{P_{39}} + r_{34}P_{49} + r_{35}P_{59} + r_{36}P_{69} + r_{37}P_{79} + r_{38}P_{89} \tag{3}$$

$$r_{49} = r_{14}P_{19} + r_{24}P_{29} + r_{34}P_{39} + \boldsymbol{P_{49}} + r_{45}P_{59} + r_{46}P_{69} + r_{47}P_{79} + r_{48}P_{89} \tag{4}$$

$$r_{59} = r_{15}P_{19} + r_{25}P_{29} + r_{35}P_{39} + r_{45}P_{49} + \boldsymbol{P_{59}} + r_{56}P_{69} + r_{57}P_{79} + r_{58}P_{89} \tag{5}$$

$$r_{69} = r_{16}P_{19} + r_{26}P_{29} + r_{36}P_{39} + r_{46}P_{49} + r_{56}P_{59} + \boldsymbol{P_{69}} + r_{67}P_{79} + r_{68}P_{89} \tag{6}$$

$$r_{79} = r_{17}P_{19} + r_{27}P_{29} + r_{37}P_{39} + r_{47}P_{49} + r_{57}P_{59} + r_{67}P_{69} + \boldsymbol{P_{79}} + r_{78}P_{89} \tag{7}$$

$$r_{89} = r_{18}P_{19} + r_{28}P_{29} + r_{38}P_{39} + r_{48}P_{49} + r_{58}P_{59} + r_{68}P_{69} + r_{78}P_{79} + \boldsymbol{P_{89}} \tag{8}$$

where r_{ij} is the simple correlation coefficient between the P fractions and the resin Pi, P_{ij} are the path

coefficients (direct effect), and $r_{ij}P_{ij}$ are the indirect effects of the P fractions on the resin Pi. The subscripts are (1) bicarbonate Pi, (2) bicarbonate Po, (3) hydroxide Pi, (4) hydroxide Po, (5) sonic Po, (6) HCl Pi, (7) HCl P_{hot}, (8) residual P, and (9) resin Pi. The model residual (U) was calculated using the following equation:

$$U = \sqrt{1 - R^2}$$

where R^2 is the determination coefficient. The correlation, multiple regression, and path analyses were done using the software SAEG 8.0 (SAEG Inst. Inc.).

Exploratory factor analysis was used to test the hypothesis that functional P pools can be distinguished (non-measurable variables—latent) based on the pattern of covariance between the P fractions. Following this system, pools of P are formed as a function of their solubility in the range of extractions represented by the Hedley procedure as described above (Gijsman et al. 1996; Novais and Smyth 1999). A basic assumption of the factor analysis is that some latent structure (pool of P) exists in the set of selected variables (P fractions), accordingly we used four factors (latent variables) considered sufficient to represent the latent structure of the data. A factor loading of ≥ 0.60 was used as a selection criterion to interpret the role that each variable (P fraction) plays in the definition of each factor (pool of P), considering the sample size of the database ($N = 81$) at a significance level of 5 %. The factor loadings are the correlation of each variable with the factor; therefore, they indicate the degree of correspondence between the variable and the factor (Hair and Anderson 2010). The factor analysis was done using the GENE 7.0 software package (GENE Inst. Inc.).

Structural equation modeling

The results of the isolated multiple regression, path, and factor analyses served as a basis for the development of candidate models of the P cycle in the soil. These models constitute null hypotheses, and the method of SEM was used for model evaluation. SEM is included in the class of generalized linear models, allowing for the simultaneous testing of a set of regression equations. As a flexible multivariate analysis method that includes factor and path analysis, SEM is ideally suited to evaluate the relative importance of the pathways in hypothetical models and to compare models with experimental data (Mulaik 2009; Allison et al. 2007). The SEM variables are classified into two major groups according to two criteria. The variables may be observable (P fractions) or latent (pools of P). The former are based on direct measurement, while the latter are identified only by their effect on the observable variables. The latent variable (or structural) model specifies the causal relationships among the latent variables, enabling the study of the interdependence between the variables, including the determination of whether they are related (Arhonditsis et al. 2006). In addition, this model also allows for testing of the indirect effects that may be mediated by another intermediate variable (Doblas-Miranda et al. 2009).

Structural equation modeling diagrams typically use two symbols to indicate the relationship between different variables: a single arrow, which indicates a direct action or causal relation of the variable from which the arrow departs (exogenous variable) on the variable to which the arrow points (endogenous variable), or a double arrow, indicating a covariance between the variables involved. Because one of the goals of SEM is to determine the regression coefficients for each of these relationships, each endogenous variable in the model and each arrow that points to it are considered. As a result, we obtain a set of equations, namely structural equations that, in turn, will produce a system of linear equations in which the unknown factors are the coefficients of multiple regressions (Kline 2005; Mulaik 2009).

For testing hypothetical models of the P cycle, at the exploratory level, we first designed a preliminary basic structural model (Model generating) with five latent variables to evaluate the relative importance of P pools affecting the soil available P. These included the organic pool, the inorganic pool, the occluded pool and the primary mineral pool as exogenous variables, and the available pool as an endogenous variable (Fig. 1). The exploratory analysis of the basic hypothesized structural model was done in five steps, according to Malaeb et al. (2000): (1) model specification, (2) model identification, (3) parameter estimation, (4) testing model fit, and (5) re-specification of the model. Thus, the basic model was split into two sub-models and tested again using the same data. The goal in this process is to obtain a model that is consistent with the data based on comparisons between the covariances in the data and those implied

by the model (Travis and Grace 2010). The matrix representation of the structural equation models is shown in the Appendix 2.

The SEM was implemented using the software AMOS v 21.0 (IBM; SPSS Inc., Chicago, IL, USA). We used the method of Maximum Likelihood to estimate the parameters, and to assess the general model fit, we applied the Chi square test (χ^2). Because of the Chi square test's sensitivity to sample size, the Goodness-of-Fit Index (GFI), the comparative fit index (CFI), the Akaike Information Criterion (AIC) and the root mean square error of approximation (RMSEA) were also considered as alternative measures of model fit (Malaeb et al. 2000; Grace 2006), assuming that the observed variables follow a multivariate normal distribution. Both univariate and multivariate normality were tested (skewness and kurtosis), followed by appropriate transformations of all of the observed variables; namely, we used the Log_{10} transformation for the resin Pi, bicarbonate (Pi and Po), sonic Po, and HCl Pi fractions, and we used the $Log\ (x + 1)$ transformation for the hydroxide P (Pi and Po), HCl P$_{hot}$, and residual P fractions. The multivariate kurtosis was assessed using the Mardia test (Mardia 1974). In the χ^2 test, if the null hypothesis was not rejected (P values >0.05), the model was assumed to have a good fit. The RMSEA values less than 0.07 suggest an adequate model fit, and similarly in the AIC index the preferred model is the one with the lowest value, while in the GFI and CFI indices the cut-off criterion ≥0.95 is indicative of good fit (Hooper et al. 2008).

Results and discussion

Factor and path analysis

The soils used here exhibited a wide variation in chemical and physical properties (see Appendix Table 8) and in P concentrations (Table 1). This variation allowed use of correlation and regression analyses to assess how the P fractions vary in relation to soil properties and to determine the interrelationships between the different P fractions. pH values are positively related to the changes in total soil N and organic C but are negatively related to the levels of Fe and Al oxides. Carbon shows a weak relationship with clay. In contrast, Fe and Al are closely related to the variation in clay content (see Appendix Table 9).

Table 1 Soil phosphorus fractions values of the literature survey

	Mean	SD	Max.	Min.	N
Resin Pi (mg kg^{-1})	6.4	7.5	34.3	0.2	81
NaHCO$_3$ Pi (mg kg^{-1})	8.5	11.8	58.8	0.1	81
NaHCO$_3$ Po (mg kg^{-1})	15.7	17.2	103	0.2	81
NaOH Pi (mg kg^{-1})	34.8	56.2	437	0.1	81
NaOH Po (mg kg^{-1})	64.8	77.7	496	4.1	81
Sonic Pi (mg kg^{-1})	7.6	7.7	39	1.0	81
Sonic Po (mg kg^{-1})	19.8	20.1	101	3.4	81
HCl Pi (mg kg^{-1})	13.1	22.3	143	0.5	81
HCl P$_{hot}$ (mg kg^{-1})	104	134	1,043	4.2	81
Residual P (mg kg^{-1})	119	118	626	4.2	81
Total Po (mg kg^{-1})	100	111	692	14	81
Total P (mg kg^{-1})	394	400	2,458	60	81

SD standard deviation, *Max.* maximum value, *Min.* minimum value, *N* soil samples number

The interactions between the different P fractions and other soil properties were also evaluated with correlation analysis (Table 2). This analysis revealed a close relationship of the organic P fractions with organic C and total N, and positive relationships with the pH and clay content. Additionally, organic C, total N, and pH also have a positive influence on the inorganic P fractions. The resin Pi is negatively correlated with the Fe oxide content. Turner and Engelbrecht (2011), using NaOH–EDTA extraction and solution 31P nuclear magnetic resonance spectroscopy in soils under tropical forest in Panama, found close and positive associations of the total soil inorganic and organic P with soil pH and total soil C, but clay content did not appear to influence the contents of soil organic P as determined by simple correlations. However, Harrison (1987) reported weak relationship between organic C and organic P in tropical soils unlike temperate soils.

Another analysis using multiple regressions of the selected variables shows that only the contents of organic C and total N had significant direct effects on most of the P fractions (see Appendix Table 10). The accumulation of organic C results in an increase in sonic Po at the expense of labile Po (bicarbonate Po). Resin Pi and hydroxide Pi were also positively related to organic C. The total N content was related to the reduction of bicarbonate Pi and hydroxide Pi amounts but increased Po amounts (bicarbonate and hydroxide). The clay content and pH had an insignificant

Table 2 Pearson correlation coefficients between P fractions and selected soil properties

	pH	C	N	Fe_{ox}	Al_{ox}	Clay
Resin Pi	0.51***	0.54***	0.71***	−0.57*	−0.49[†]	0.22[†]
NaHCO₃ Pi	0.42***	0.48***	0.48***	−0.46[†]	−0.33[†]	0.11[†]
NaHCO₃ Po	0.33**	0.74***	0.81***	−0.46[†]	−0.34[†]	0.30*
NaOH Pi	0.29**	0.48***	0.45**	−0.33[†]	−0.17[†]	0.11[†]
NaOH Po	0.45***	0.75***	0.83***	−0.31[†]	−0.19[†]	0.42**
Sonic Po	0.44***	0.69***	0.78***	−0.44[†]	−0.31[†]	0.34*
HCl Pi	0.57***	0.07[†]	0.31*	−0.60*	−0.57*	−0.07[†]
HCl P_hot	0.18[†]	0.35***	0.39*	−0.48[†]	−0.36[†]	0.32*
Residual P	0.34**	0.53***	0.73***	−0.56*	−0.50*	0.20[†]

Significant at *** $P < 0.001$; ** $P < 0.01$; * $P < 0.05$; [†] no significant

Table 3 Pearson correlation coefficients for nine soil P fractions (All the coefficients are significant at $P < 0.001$)

	NaHCO₃ Pi	NaHCO₃ Po	NaOH Pi	NaOH Po	Sonic Po	HCl Pi	HCl P_hot	Residual P
Resin Pi	0.71	0.55	0.68	0.80	0.86	0.65	0.67	0.71
NaHCO₃ Pi		0.46	0.79	0.58	0.73	0.64	0.51	0.59
NaHCO₃ Po			0.27	0.85	0.72	0.30	0.43	0.63
NaOH Pi				0.50	0.75	0.49	0.55	0.67
NaOH Po					0.89	0.42	0.61	0.73
Sonic Po						0.54	0.80	0.87
HCl Pi							0.43	0.42
HCl P_hot								0.77

effect on all of the P fractions. No significant direct effects of the soil properties were found on HCl Pi, HCl P_hot, and residual P amounts. The total organic P fraction (bicarbonate, hydroxide, and sonic) was positively related to the soil properties, but only the total N had a direct effect on this fraction.

Table 3 shows the interrelationships of the different P fractions as determined by simple correlations. Close associations are observed between the P fractions. These Pearson correlation coefficients were comparable with those reported by Negassa and Leinweber (2009) for subtropical and tropical soils. However, detailed information regarding the interactions between the different fractions cannot be obtained from a simple correlation analysis. Factor analysis can reduce the dimensionality of the problem by using fewer latent or unobserved variables to explain variation in the measured variables. Thus, using factor analysis we obtained four factors that conceptually clarify the grouping of P fractions (Table 4): factor 1 represents all of the Po fractions, factor two represents the Pi fraction of the primary

Table 4 Factor analysis of soil P in different fractions

	Factor			
	1	2	3	4
Factor loading[†]				
Resin Pi	–	0.92	–	–
NaHCO₃ Pi	–	–	–	0.75
NaOH Pi	–	–	–	0.97
NaHCO₃ Po	0.99	–	–	–
NaOH Po	0.86	–	–	–
Sonic Po	0.65	–	–	–
HCl Pi	–	0.99	–	–
HCl P_hot	–	–	0.98	–
Residual P	–	–	0.62	–

[†] Only loadings ≥60 % of the maximum are given

minerals, factor three represents the occluded P fractions, and factor 4 represents the Pi fraction of the secondary minerals. Similar results were reported by Tiessen et al. (1984) for temperate soils.

Table 5 Path analysis direct effects (diagonal, bold) and indirect effects (off-diagonal) of different soil P fractions on resin Pi

	NaHCO$_3$ Pi	NaHCO$_3$ Po	NaOH Pi	NaOH Po	Sonic Po	HCl Pi	HCl P$_{hot}$	Residual P	r
NaHCO$_3$ Pi	**0.10**	−0.18	−0.05	0.34	0.37	0.15	−0.02	<0.01	0.71
NaHCO$_3$ Po	0.05	**−0.39***	−0.02	0.50*	0.36	0.07	−0.01	<0.01	0.56
NaOH Pi	0.08	−0.10	**−0.06**	0.30	0.37	0.11	−0.02	<0.01	0.68
NaOH Po	0.06	−0.33	−0.03	**0.59***	0.44*	0.09	−0.02	<0.01	0.80
Sonic Po	0.07	−0.28	−0.05	0.52*	**0.50***	0.12	−0.03	<0.01	0.86
HCl Pi	0.06	−0.11	−0.03	0.25	0.27	**0.23**	−0.01	<0.01	0.65
HCl P$_{hot}$	0.05	−0.17	−0.03	0.36	0.40*	0.10	**−0.03**	<0.01	0.67
Residual P	0.06	−0.24	−0.04	0.43*	0.44*	0.09	−0.02	**<0.01**	0.71

$U = 0.39$

Significant at * $P < 0.05$

$R^2 = 0.85$ ($P < 0.05$)

r ($P < 0.001$)

The relationships between the resin Pi fraction and the other P fractions were evaluated using a series of multiple regressions in a path analysis (Table 5). Only the fractions of organic P (bicarbonate Po, hydroxide Po, and sonic Po) had a significant direct influence on the resin Pi fraction. Of these fractions, only the organic fraction of bicarbonate Po showed a negative effect. Furthermore, the bicarbonate Po, sonic Po, and residual P fractions had a significant positive indirect influence on the resin Pi fraction via the hydroxide Po fraction. Similarly, the hydroxide Po, HCl P$_{hot}$, and residual P fractions had a significant positive indirect influence on the resin Pi via the sonic Po fraction.

In the backward regression model only the bicarbonate Po, hydroxide Po, sonic Po, and HCl Pi fractions were identified as statistically significant for predicting resin Pi fractions, with a coefficient of determination (R^2) of 0.84 and a residue (U) of 0.40. The fractions of organic P explain 71 % of the variation in the resin Pi fraction (see Appendix Table 11).

Backward stepwise regression analysis was used to decompose the correlation coefficients between the resin Pi and P fractions into direct and indirect effects (Table 6). The effect of bicarbonate Po on resin Pi ($D = 0.35$) was negative and not significant. The significant positive correlations found in the correlation analysis (Table 3) between bicarbonate Po and resin Pi and between sonic Po and resin Pi were attributed to the significant indirect effect of hydroxide Po ($D = 0.51$ and 0.53, respectively; Table 6). Although all of the P fractions analyzed were

Table 6 Path analysis direct effects (diagonal, bold) and indirect effects (off-diagonal) of organic P fractions and HCl Pi on resin Pi

	NaHCO$_3$ Po	NaOH Po	Sonic Po	HCl Pi	r
NaHCO$_3$ Po	**−0.35**	0.51*	0.32	0.08	0.55
NaOH Po	−0.30	**0.60***	0.40	0.11	0.80
Sonic Po	−0.25	0.53*	**0.45***	0.14	0.86
HCl Pi	−0.10	0.25	0.25	**0.26**	0.65

$U = 0.40$

Significant at * $P < 0.05$

$R^2 = 0.84$ ($P < 0.05$)

r ($P < 0.001$)

significantly related to the resin Pi, only hydroxide Po and sonic Po had significant direct effects on the resin Pi, and hydroxide Po had the highest direct effect ($D = 0.60$).

Structural equation modeling

The multiple regression, factor, and path analyses were able to distinguish between the direct and indirect effects of the soil properties on the P fractions, as well as to support a hypothetical distinction between the pools of P in the soil. When these statistical techniques are used in combination with the method of SEM, the levels of interdependence between the pools of P are quantified, and thus, the cause and effect relationship related to the

Fig. 2 Model *A*, structural equation model for the soil P cycle. All measured variables (in *boxes*) are represented as effect indicators associated with latent variables (in *circles*). The numbers correspond to the standardized parameters estimated ($P < 0.001$). Error variables ($\varepsilon_1 - \varepsilon_9$ *and* ζ_1) are standardized values. Model $\chi^2 = 165.61$, $df = 17$, $P < 0.0001$
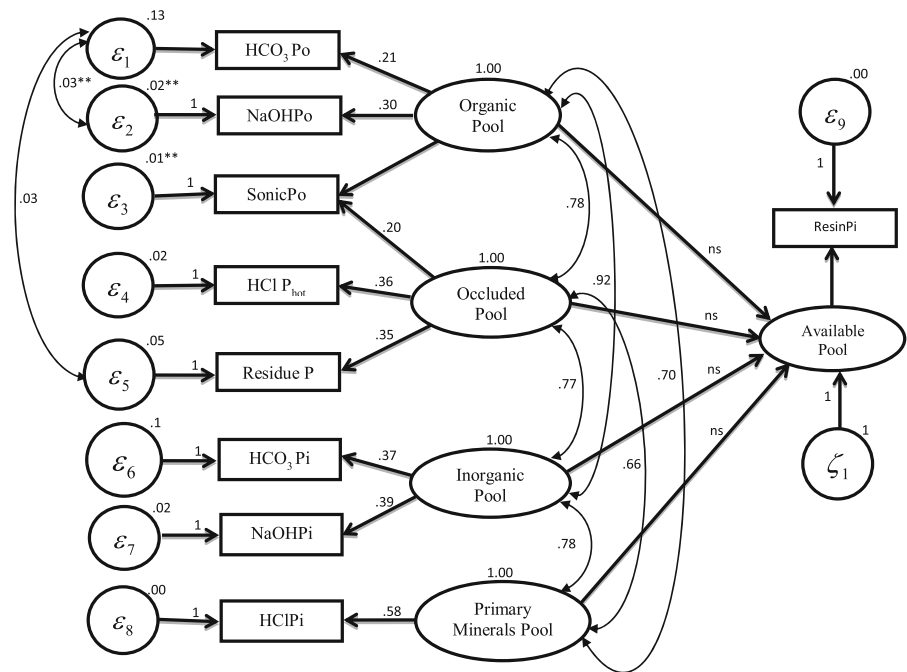
transformation pathway of the element in the soil can be inferred. Figures 2 and 3 show the versions of the structural model of the P cycle based on factor analysis. The biological and geochemical processes of P in the soil are shown in the conceptual model *A,* in which all of the organic P fractions are grouped in the organic pool and all of the inorganic labile fractions are grouped in the inorganic P pool. The recalcitrant fractions (also included the sonic Po fraction) are associated with the occluded pool, the HCl Pi fraction is associated with the primary mineral pool, and the resin Pi fraction constitutes the most exchangeable pool (Fig. 2). Model *A* showed an unsatisfactory overall adjustment based on the Chi square test ($\chi^2 = 165.61$, $df = 17$, $P < 0.0001$) and the other tests (GFI = 0.818; CFI = 0.777; CFI = 0.818; AIC = 221; RMSEA = 0.331). Conversely, all of the regression coefficients between the measured variables (P fractions) and the latent variables (pools of P) were highly significant ($P < 0.001$), which implies that all of the P fractions were appropriate indicators of the pools of P, demonstrating a plausible causality structure via the SEM method. Moreover, the close relationship between the P fractions and the pools of P reveals the functional nature of these pools when one considers that no clear boundaries exist between the quantified P fractions by the method of sequential extraction. The covariance values of all of

the P pools (exogenous latent variables) were also highly significant ($P < 0.001$), but the regression coefficients of the relationship of these P pools with the resin P (endogenous latent variables) were not significant. The high covariance between the P pools (exogenous latent variables) affected the relationship of each of these pools with the most exchangeable P pool, yielding an overall apparently null effect for all of the P sources.

We evaluated the different sub-models assuming that at least one of the P sources should have a significant relationship with the resin P pool. Model *B* is a simplified version of the complete structural model, consisting only of the organic and occluded pools as exogenous variables (Fig. 3). In this model, the regression coefficient of the relationship between the organic pool and the resin P pool was significant ($P = 0.003$). In contrast, model *B* also showed an unsatisfactory overall fit ($\chi^2 = 105.13$, $df = 7$, $P < 0.0001$; GFI = 0.842; CFI = 0.761; AIC = 133; RMSEA = 0.419).

Model *C*, a variation of model *B* shown in Fig. 4, illustrates the logical dependency between the P fractions (measurable variables) and available P pool (endogenous latent variable). This model is a latent variable model with single indicator (Resin Pi) and it is not saturated, as not all of the paths are specified, and represents a testable hypothesis. The general fit of the

Fig. 3 Model *B*, structural equation model for the soil P cycle. All measured variables (in *boxes*) are represented as effect indicators associated with latent variables (in *circles*). The numbers correspond to the standardized parameters estimated ($P < 0.001$). *Double asterisks* significant at $P < 0.01$. Error variables ($\varepsilon_1 - \varepsilon_6$ *and* ζ_1) are standardized values. Model $\chi^2 = 105.13$, $df = 7$, $P < 0.0001$
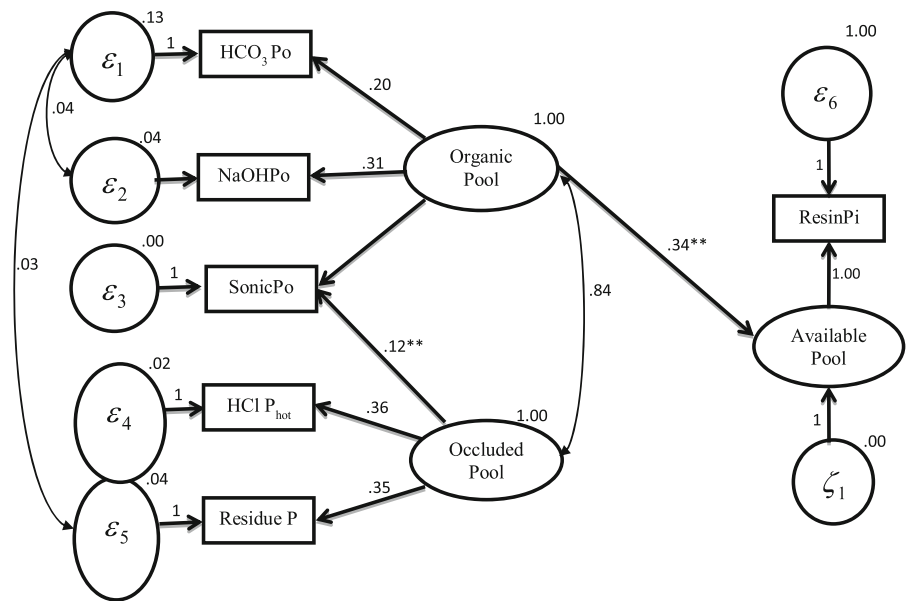

model was satisfactory ($\chi^2 = 3.44$, $df = 3$, $P = 0.329$; GFI = 0.986; CFI = 0.999; AIC = 39; RMSEA = 0.043). All the regression coefficients of the relationships between the P fractions were significant. The available P pool was directly dependent on the organic P fractions ($P < 0.05$). The hydroxide Po and sonic Po fractions had a positive direct effect, and the overall effect of sonic Po was greater [$\beta = 1.67 + (1.88 \times 0.95) = 3.46$] than the direct effect of that fraction. The bicarbonate Po had a direct negative effect and indirect positive effect via hydroxide Po and sonic Po on the available P pool, but its overall positive effect was low [$\beta = (0.37 \times 1.88) + (0.11 \times 1.67) + (0.11 \ x \ 1.67 \times 1.88) - 0.91) = 0.17$]. The indirect effects of the recalcitrant fractions were complex. The residual P had a negative effect via hydroxide Po and a positive effect via sonic Po, but its indirect overall effect was positively very low [$\beta = (-0.28 \times 1.88) + (0.20 \times 1.67) + (0.20 \times 0.95 \times 1.88) = 0.16$]. In contrast, HCl P_{hot} showed high overall positive effect [$\beta = (0.55 \times 1.67) + (0.55 \times 0.95 \times 1.88) = 1.90$]. The residual P had an overall negative effect on hydroxide Po very low [$\beta = (0.20 \times 0.95) - 0.28 = -0.09$].

The model *C* (Fig. 4) of the P cycle fitted by the SEM method is theoretically consistent and is likely general, considering that the present study is a comprehensive analysis at an exploratory level of the P fractions in a range of unfertilized tropical soils, but this model needs confirmation using independent data.

The weak overall adjustment of the tested structural models *A* and *B* (Figs. 2, 3) highlights the need for future studies to improve the adequacy of these models or that they are simply inadequate. However, it should be noted that a well-adjusted model is not necessarily a valid model (Kenny 2012). A good general fit only shows that the model adequately describes the observed data (Mitchell 1992). A model that is not well adjusted can have parameters that are all statistically significant (Kenny 2012). In this case, within certain limits, the hypothetical model can be used to describe the relationships between the variables that comprise it (Fig. 3), where the regressions of these relationships are evaluated simultaneously, allowing for the comparison of the relative importance of the indicator variables (Malaeb et al. 2000). Moreover, the close correlation between the measurable variables (P fractions, Table 3) and the covariance between the latent variables (P pools) affects the overall degree of fit of the hypothetical structural models evaluated by the χ^2 test (Figs. 2, 3). This type of overall fit index is affected by the size of the correlations in the model. Large correlations result in low fit indices (Kenny 2012). Thus, we must consider that this is perhaps a problem inherent to the structural models of P fractions in the soil, based on the sequential extraction method. In this method, the P fractions are not true independent variables. Thus, given that the variables that contribute the most to any high collinearity of the data are discarded, the hypothetical model of the P

Fig. 4 Model C, structural equation model for the soil P cycle. Hypothesized model relating labile and stable P fractions (measured variables) to available P pool (latent variable). The numbers correspond to the standardized parameters estimated ($P < 0.001$) and the R-squared values (*numbers in bold*). Asterisk, *double asterisk* significant at $P < 0.05$ and 0.01 respectively. Error variables ($\varepsilon_1 - \varepsilon_3$ *and* ζ_1) are standardized values. Model $\chi^2 = 3.42$, $df = 3$, $P < 0.329$
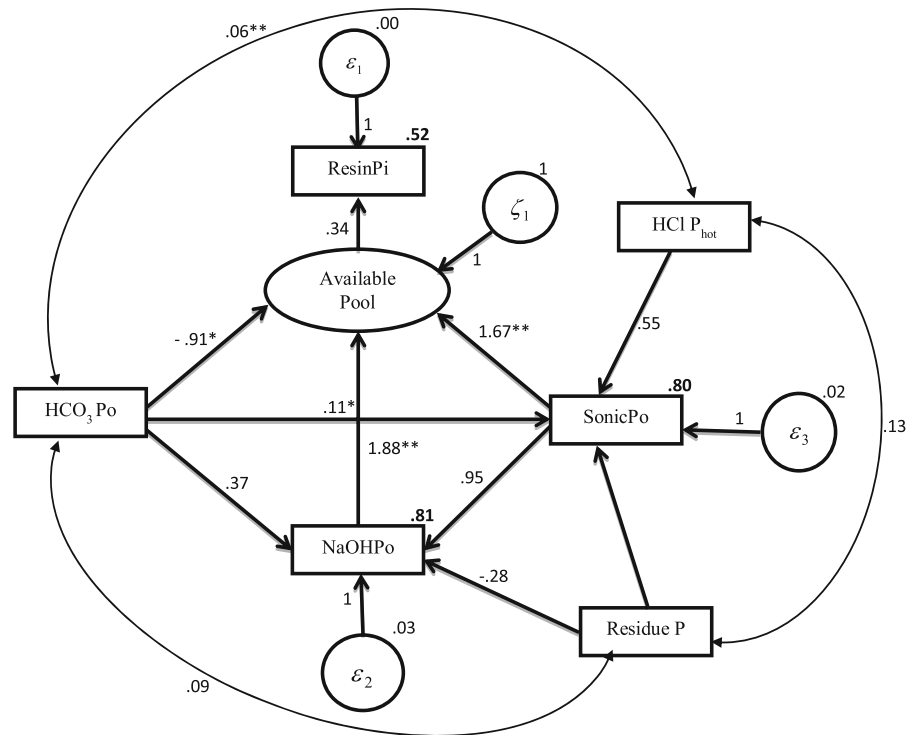
cycle can be evaluated using the set of regression coefficients to make inferences about the direction and strength of relationship between their variables, as obtained using the SEM method (Tiessen et al. 1984; Beck and Sanchez 1994; Zheng et al. 2002).

Our analysis of the P cycle models, based on all of the statistical techniques, showed that the resin Pi (indicator of available P pool) was closely related to the Po fractions. Thus, there is strong support for the control of available P pool by the mineralization of organic P, from which the moderately stable fraction of hydroxide Po acts as the primary source of available P pool and as a transitional fraction of the other Po fractions. In model C (Fig. 4), the labile bicarbonate Po seems to act as a sink of available P pool, considering the dependency of available P pool with respect only to the organic P fractions (indicators of organic P pool). The sonic Po is also revealed as a fraction with an important role in the overall dynamics of P in tropical soils, although this fraction is considered as the recalcitrant/stable form of Po (Cross and Schlesinger 1995). This fraction showed a close relationship with the other recalcitrant P fractions in the soil. In part, this may occur because the HCl P_{hot} and residual P fractions have a considerable and very stable Po content (Tiessen and Moir 1993; Cross and

Schlesinger 1995; Oberson et al. 2001; Linquist et al. 1997; Frizano et al. 2002, 2003; Giardina et al. 2000).

In general, the total organic P made up 25.5 % of the total P, and the average proportion of the hydroxide Po of the total organic P was 64.5 % (Table 1). Other studies reported similar values of the proportion of organic P (24.9–28.7 %) in strongly weathered soils, determined by both ignition and extraction procedures (Sharpley et al. 1987; Harrison 1987; Turner and Engelbrecht 2011). Using path models, Tiessen et al. (1984) and Beck and Sanchez (1994) showed that in highly weathered Ultisols, 44–80 % of the variation in resin P was explained by the organic fractions (bicarbonate and hydroxide). Soil organic P is a major source of plant-available P in low input tropical agriculture and forests (Negassa and Leinweber 2009; Reed et al. 2011). The transformation pathway of P in the soil, especially the magnitude of influence of the organic P on the available P, depends on the type of soil, climate, type of P sources and land use history. But as a number of factors contribute to transformations of P fractions, it is difficult to exactly determine the kinetics of exchange reactions (Negassa and Leinweber 2009).

The models tested in this study may be used like tool in understanding of some processes of P cycling in

determining the function and productivity of tropical forest and perennial plants, considering that the Ultisols and Oxisols are the dominant tropical orders and are characterized by relatively low P availability (Reed et al. 2011). As occluded pool of P was the sparingly available P and organic pool of P was considered reversibly available (Model C, Fig. 4), the uptake of P by plants would be regulated by the turnover of organic P and the rapid recycling of P from accumulated litter (Turner and Engelbrecht 2011). However, what is the real contribution of soil organic P to the nutrition of ecosystems is not yet known. Therefore, further research is now required to refine the model C (Fig. 4) to maximize the efficiency of P use in low-input agricultural systems.

Conclusion

We proposed and analyzed conceptual models of P cycling in unfertilized tropical soils, finding that the organic P pool constitutes the main source of available

P pool with resin P fraction as its single indicator. This result implies that caution should be used in low-input agricultural systems, when using conventional methods of soil fertility analysis that are not sensitive enough to detect changes in the forms of soil P.

Structural equation modeling proved to be a suitable tool with which to understand the various possible cycles of P in the tested soils, indicating the degree to which the alterations in the P level of a pool can affect the other P pools. Thus, SEM can be used not only to evaluate hypotheses but also to help improve them in an exploratory manner.

Appendix 1

Table 7 Studies using sequential phosphorus fractionation for tropical soils under different land use type

Reference	Cover	Soil type	Location
Szott and Melendez (2001)	Native forest	Typic Humitropept (Inceptisol)	Costa Rica
	Native forest	Typic Paleudult (Ultisol)	Peru
	Alley cropping/Multistrata agroforest		
Lehmann et al. (2001)	Native forest	Typic Hapludox (Oxisol)	Brazil
	Secondary forest		
Garci-Montiel et al. (2000)	Native forest	Kandiudult (Ultisol)	Brazil
	Pastures (13, 20 and 41 years)		
	Native forest	Paleudult (Ultisol)	
	Pasture (20 years)		
Solomon and Lehmamn (2000)	Native woodland	Chromic Luvisol	Tanzania
Solomon et al. (2002)	Native forest	Plintic Alisol	Ethiopia
	Native forest	Humic Nitisol	
Frizano et al. (2002)	Secondary forest (16, 30, 51, 66, 300 years)	Oxisols, Ultisols and Inceptsols	Puerto Rico
Frizano et al. (2003)	Native forest	Oxisol (Yellow Latosol)	Brazil
	Secondary forest (10, 20 and 40 years)		
Giardina et al. (2000)	Native forest	Typic Ustorthents	Mexico
Kitayama et al. (2000)	Native forest	Sedimantary substrate and ultrabasic substrate	Borneo
Möller et al. (2000)	Native forest	Humic Cambisol	
	Secondary forest (15 years)	Skeletic Umbrisol	
	Pinus kesiya (20 years)	Dystric Cambisol	Thailand

Table 7 continued

Reference	Cover	Soil type	Location
Olander et al. (2005)	Native forest	Oxisol	Brazil
Newbery et al. (1997)	Native forest		Cameroon
Beck and Sanchez (1994)	Secondary forest (17 years)	Typic Paleudult (Ultisol)	Peru
Leite (2001)	Secondary forest	Oxisols (Red Yellow Latosol, Red Latosol) and Cambisol	Brazil
	Eucalyptus grandis (21 years)		
	Pasture		
Lilienfein et al. (2000)	*Eucalyptus grandis*	Oxisols	Brazil
	Pinus caribaea		
	Native savanna		
Neufeldt et al. (2000)	Native savanna	Anionic Acrustox (Oxisol)	Brazil
	Pinus caribaea		
	Native savanna	Typic Haplustox	
	Eucalyptus citriodora		
Tchienkoua and Zech (2003)	*Eucalyptus grandis*	Andic Palehumult	Cameroon
Cardoso et al. (2003)	Coffee agroforest	Oxisol	Brazil
Araújo et al. (2004)	Native xerophytic vegetation	Latosols and Luvisols	Brazil
Tiessen et al. (1992)	Thorn bush savana	Oxisol (Paleustox)	Brazil
Agbenin and Goladi (1998)	Native savanna	Typic Haplustalf (Alfisol)	Nigeria
Oberson et al. (2001)	Native savanna	Tropeptic Haplustox (Oxisol)	Colombia
Linquist et al. (1997)	Pasture (45 years)	Typic Palehumult (Ultisol)	Hawaii

Table 8 Selected chemical and physical soil properties values of the literature survey

	Mean	SD	Max.	Min.	N
pH	5.0	0.8	7.6	3.5	62
C (g kg^{-1})	23.0	18.7	103.0	0.8	70
N (g kg^{-1})	2.2	2.0	8.2	0.3	34
Fe$_{ox}$ (g kg^{-1})	17.3	15.2	42.2	1.0	12
Al$_{ox}$ (g kg^{-1})	1.5	1.4	4.7	0.4	12
Clay (g kg^{-1})	318	224	800	62	35

SD standard deviation, *Max.* maximum value, *Min.* minimum value, *N* soil samples number

Table 9 Pearson correlation coefficients between different selected soil properties

	pH	C	N	Fe$_{ox}$	Al$_{ox}$	Clay
pH	1	0.24*	0.53**	−0.95***	−0.91***	−0.25[†]
C			0.97**	−0.19[†]	−0.07[†]	0.38*
N				−0.70[†]	−0.72[†]	0.17[†]
Fe$_{ox}$					0.95**	0.66**
Al$_{ox}$						0.77**

Significant at *** $P < 0.001$; ** $P < 0.01$; * $P < 0.05$; [†] no significant

Table 10 Multiple regressions of P contained in different fractions with selected soil properties

	β (direct effect)				R^2
	pH	C	N	Clay	
Resin Pi	0.186[†]	1.163*	−0.589[†]	0.194[†]	0.61 ($P \leq 0.01$)
NaHCO$_3$ Pi	0.301[†]	1.528*	−1.233*	0.004[†]	0.39 ($P > 0.05$)
NaHCO$_3$ Po	0.170[†]	−1.439*	2.112*	0.159[†]	0.78 ($P \leq 0.001$)
NaOH Pi	−0.208[†]	2.649*	−1.984*	−0.223[†]	0.45 ($P \leq 0.05$)
NaOH Po	0.138[†]	0.209	0.525*	0.251[†]	0.80 ($P \leq 0.001$)
Sonic Po	0.053[†]	0.650*	0.120	0.114[†]	0.69 ($P \leq 0.001$)
HCl Pi	0.665[†]	−1.230*	1.001*	0.292[†]	0.29 ($P > 0.05$)
HCl P$_{hot}$	0.008[†]	−0.273[†]	0.584[†]	0.217[†]	0.17 ($P > 0.10$)
Residual P	−0.299[†]	0.401[†]	0.537[†]	−0.008[†]	0.60 ($P \leq 0.01$)
Total Po	0.133[†]	0.051[†]	0.710*	0.223[†]	0.82 ($P \leq 0.001$)

Significant at * $P \leq 0.05$; [†] no significant

Table 11 Multiple regression of resin Pi with organic P fractions and HCl Pi

	Regression coefficients	β (direct effects)
NaHCO$_3$ Po	−0.153053 ($P < 0.00001$)	−0.352
NaOH Po	0.0575956 ($P < 0.0001$)	0.598
Sonic Po	0.167571 ($P < 0.0001$)	0.449
HCl Pi	0.0874324 ($P < 0.0001$)	0.260
Constant	0.560753	
R^2	0.844 ($P < 0.00001$)	
U	0.394	
Contribution to R^2 (%)		
NaHCO$_3$ Po	22	
NaOH Po	26	
Sonic Po	23	
HCl Pi	29	

Appendix 2

The general matrix representation of structural equation models

Structural equations modeling (SEM) is included in the Generalized Linear Models class, which allows the simultaneous test of a set of regression equations. In order to obtain those equations, a fundamental assumption is made: all equations relating the latent and manifest, exogenous or endogenous variables are linear.

We will examine the matrix equations derived from the basic hypothesized model (Fig. 1) and model C (Fig. 4).

In order to write the structural equations in matrix representation, first we obtain the vectors of endogenous and exogenous variables as well as disturbances,

then the structural coefficients matrices. Each vector is partitioned in blocks of latent and manifest variables, as shown below:

$$\begin{bmatrix} N \\ Y \\ X \end{bmatrix} = \begin{bmatrix} \Gamma \\ \Lambda_y \\ \Lambda_x \end{bmatrix} \begin{bmatrix} Z \\ N \end{bmatrix} + \begin{bmatrix} \Delta & 0 \\ 0 & \Psi \end{bmatrix} \begin{bmatrix} \Xi \\ E \end{bmatrix}, \qquad (9)$$

where N is a vector of the latent endogenous variables η, Y is a vector of the manifest endogenous variables y, X is a vector of the manifest endogenous variables x, Γ is a matrix of structural coefficients relating latent exogenous variables to latent endogenous variables, Λ_y is a matrix of structural coefficients relating manifest endogenous variables y to latent endogenous variables, Λ_x is a matrix of structural coefficients relating manifest endogenous variables x to latent exogenous

variables, Z is a vector of the latent exogenous variables, and Ξ and E are vectors of disturbances of latent and manifest endogenous variables, respectively.

Matrices and vectors in basic hypothesized model (Fig. 1)

In this model, there are:

(a) Latent endogenous variables: The most available P pool
(b) Latent exogenous variables: Organic P pool, Primary minerals pool, Occluded P pool, Inorganic P pool.
(c) Disturbance related to latent endogenous variables: ζ_1.

Structural equation:

$$\eta_1 = \gamma_{1,1}\xi_1 + \gamma_{1,2}\xi_2 + \gamma_{1,3}\xi_3 + \gamma_{1,4}\xi_4 + \zeta_1 \qquad (10)$$

where $\eta_1 \rightarrow$ Available pool
$\quad \xi_1 \rightarrow$ Organic Pool
$\quad \xi_2 \rightarrow$ Occluded Pool
$\quad \xi_3 \rightarrow$ Inorganic Pool
$\quad \xi_4 \rightarrow$ Primary minerals Pool

Matrix:

$$[N] = [\Gamma][Z] + [\Delta][\Xi], \qquad (11)$$

where, $N = [\eta_1]$, the vector of manifest endogenous variable. Γ is the block matrix $\begin{bmatrix} \gamma_{1,1} & \gamma_{1,2} & \gamma_{1,3} & \gamma_{1,4} \end{bmatrix}$ of structural coefficients matrix relating just the latent exogenous variables to the latent endogenous variable η_1.

$$Z = \begin{bmatrix} \xi_1 \\ \xi_2 \\ \xi_3 \\ \xi_4 \end{bmatrix}, \text{ the vector of latent exogenous}$$

variables.

$\Delta = [1]$, the 1×1 matrix of disturbance related to the latent endogenous variable η_1.

$\Xi = [\zeta_1]$, the vector of disturbance related to latent endogenous variable.

So that, (Eq. 12) becomes:

$$[\eta_1] = \begin{bmatrix} \gamma_{1,1} & \gamma_{1,2} & \gamma_{1,3} & \gamma_{1,4} \end{bmatrix} \begin{bmatrix} \xi_1 \\ \xi_2 \\ \xi_3 \\ \xi_4 \end{bmatrix} + [1][\zeta_1],$$

$$(12)$$

Matrices and vectors in model C (Fig. 4)

Now, in this model we have:

(a) Latent endogenous variables in the model: Available Pool
(b) Manifest endogenous variables in the model: Resin Pi, NaOH Po, Sonic Po.
(c) Latent exogenous variables in the model: none
(d) Manifest exogenous variables in the model: HCO_3 Po, HCl P_{hot}, Residual P.
(e) Disturbance related to latent endogenous variables: ζ_1
(f) Disturbance related to manifest endogenous variable: $\varepsilon_1, \varepsilon_2, \varepsilon_3$

Therefore we obtain:

$$\begin{bmatrix} Y \\ N \end{bmatrix} = \begin{bmatrix} \Lambda & 0 \\ B_x & B_y \end{bmatrix} \begin{bmatrix} N \\ X \\ Y \end{bmatrix} + \begin{bmatrix} \Delta & 0 \\ 0 & \Psi \end{bmatrix} \begin{bmatrix} E \\ \Xi \end{bmatrix} \qquad (13)$$

$$Y = \begin{bmatrix} y_1 = \text{Resin Pi} \\ y_2 = \text{NaOH Po} \\ y_3 = \text{Sonic Po} \end{bmatrix}, \text{ the vector of manifest}$$

endogenous variables.

$N = [\eta_1]$, the vector of latent endogenous variable.

$\Lambda = [\lambda_{1,1}]$, the structural coefficient matrix relating latent endogenous variables to manifest endogenous variables y_1.

$$B_x = \begin{bmatrix} 0 & \beta_{1,2} & \beta_{2,2} & 0 \\ 0 & \beta_{1,3} & \beta_{2,3} & \beta_{3,3} \\ 0 & \beta_{1,1} & 0 & 0 \end{bmatrix}, \text{ the structural coeffi-}$$

cients matrix relating manifest endogenous variables x to endogenous variables y_2 and η_1.

$$B_y = \begin{bmatrix} 0 & 0 & \beta_{3,2} \\ 0 & 0 & 0 \\ 0 & \beta_{2,1} & \beta_{3,1} \end{bmatrix}, \text{ the structural coefficients}$$

matrix relating manifest endogenous variables y to endogenous variables y_2, y_3 and η_1.

$$X = \begin{bmatrix} x_1 = HCO_3Po \\ x_2 = \text{Residual P} \\ x_3 = \text{HCl Phot} \end{bmatrix}, \text{ the vector of manifest}$$

exogenous variables.

$$\Delta = \begin{bmatrix} 1 & 0 & 0 \\ 0 & 1 & 0 \\ 0 & 0 & 1 \end{bmatrix}.$$

$\Psi = [1]$, the 1×1 matrix of disturbance related to the latent endogenous variable η_1.

The 0 on the right of Ψ is a 1×3 block matrix of zeros and the down 0 to Ψ is a 3×1 block matrix of zeros.

Δ is the 3×3 identity matrix (a matrix with 3 rows and 3 columns with 1 in each position of its principal diagonal and 0 elsewhere) of disturbance related to the manifest endogenous variables.

$E = \begin{bmatrix} e_1 \\ e_3 \\ e_4 \end{bmatrix}$, the vector of disturbances related to manifest endogenous variables.

$\Xi = [\zeta_1]$.

So that, (Eq. 13) becomes:

$$\begin{bmatrix} y_1 \\ y_2 \\ y_3 \\ \eta_1 \end{bmatrix} = \begin{bmatrix} \lambda_{1,1} & 0 & 0 & 0 & 0 & 0 & 0 \\ 0 & \beta_{1,2} & \beta_{2,2} & 0 & 0 & 0 & \beta_{3,2} \\ 0 & \beta_{1,3} & \beta_{2,3} & \beta_{3,3} & 0 & 0 & 0 \\ 0 & \beta_{1,1} & 0 & 0 & 0 & \beta_{2,1} & \beta_{3,1} \end{bmatrix} \begin{bmatrix} \eta_1 \\ x_1 \\ x_2 \\ x_3 \\ y_2 \\ y_2 \\ y_3 \end{bmatrix} + \begin{bmatrix} 1 & 0 & 0 & 0 \\ 0 & 1 & 0 & 0 \\ 0 & 0 & 1 & 0 \\ 0 & 0 & 0 & 1 \end{bmatrix} \begin{bmatrix} \varepsilon_1 \\ \varepsilon_2 \\ \varepsilon_3 \\ \zeta_1 \end{bmatrix},$$

$$(14)$$

If we suppose that the covariances between latent exogenous variables, ξ, and the disturbance variables, ε, are zero, as well the covariance between manifest exogenous variables, x, and disturbance variables, we obtain the following block matrix of covariance, formed by the model structural coefficients:

$$\Theta = \begin{bmatrix} \Theta_{\xi\xi} & \Theta_{\xi x} & 0 \\ \Theta_{x\xi} & \Theta_{xx} & 0 \\ 0 & 0 & \Theta_{\varepsilon\varepsilon} \end{bmatrix}$$

Now, in order to relate the covariances between the original manifest endogenous variables, y, and manifest exogenous variables, x, with the matrix Φ, we need to extract them from block vectors $\begin{bmatrix} N \\ Y \end{bmatrix}$ and $\begin{bmatrix} \Xi \\ X \\ E \end{bmatrix}$. To accomplish it, we perform the following operations:

$$Y = \begin{bmatrix} 0 & I \end{bmatrix} \begin{bmatrix} N \\ Y \end{bmatrix} \text{ and } X = \begin{bmatrix} 0 & I & 0 \end{bmatrix} \begin{bmatrix} \Xi \\ X \\ E \end{bmatrix}.$$

Defining matrices $G_Y = \begin{bmatrix} 0 & I \end{bmatrix}$ and $G_X = \begin{bmatrix} 0 & I & 0 \end{bmatrix}$, the matricial equation is:

$$\begin{bmatrix} Y \\ X \end{bmatrix} = \begin{bmatrix} G_Y & 0 \\ 0 & G_X \end{bmatrix} \begin{bmatrix} \eta* \\ \xi* \end{bmatrix}$$
$$= \begin{bmatrix} G_Y & 0 \\ 0 & G_X \end{bmatrix} \begin{bmatrix} B^{-1}\Gamma\xi* \\ \xi* \end{bmatrix}$$
$$= \begin{bmatrix} G_Y & 0 \\ 0 & G_X \end{bmatrix} \begin{bmatrix} B^{-1} & 0 \\ 0 & I \end{bmatrix} \begin{bmatrix} \Gamma \\ I \end{bmatrix} \xi*,$$

which, after defining the block matrices $G = \begin{bmatrix} G_Y & 0 \\ 0 & G_X \end{bmatrix}$, $B*^{-1} = \begin{bmatrix} B^{-1} & 0 \\ 0 & I \end{bmatrix}$ and $\Gamma* = \begin{bmatrix} \Gamma \\ I \end{bmatrix}$, produces the following expressions:

$$\Sigma_{yy} = G_y B^{-1}\Gamma\Theta\Gamma^T(B^{-1})^T G_y^T$$

$$\Sigma_{xy} = G_x\Theta\Gamma^T(B^{-1})^T G_y^T$$

$$\Sigma_{xx} = G_x\Theta G_y^T = \Theta_{xx},$$

which are the covariance matrices for the manifest variables, therefore, formed by known terms, so that the three last expressions are true equations, although their calculations can be lengthy and tedious, in particular, the inverse matrix, B^{-1}, is usually hard to calculate. Fortunately, modern software, like AMOS, performs those calculations without the explicit derivations of the above equations.

References

Agbenin JO, Goladi JT (1998) Dynamics of phosphorus fractions in a savanna Alfisol under continuous cultivation. Soil Use Manag 14:59–64

Allison VJ, Yermakov Z, Miller RM, Jastrow JD, Matamala R (2007) Using landscape and gradients to decouple the impact of correlated environmental variables on soil microbial community composition. Soil Biol Biochem 39:505–516

Araújo MSB, Schaefer CEGR, Sampaio EVSB (2004) Soil phosphorus fractions from toposequences of semi-arid Latosols and Luvisols in northestern Brazil. Geoderma 119:309–321

Arhonditsis GB, Stow CA, Steinberg LJ, Kenney MA, Lathrop RC, Mcbride SJ, Reckhow KH (2006) Exploring ecological patterns with structural equation modeling and Bayesian analysis. Ecol Model 192:385–409

Beck MA, Sanchez PA (1994) Soil phosphorus fraction dynamics during 18 years of cultivation on a Typic Paleudult. Soil Sci Soc Am J 58:1424–1430

Cardoso IM, Janssen BH, Oenema O, Kuyper TW (2003) Phosphorus pools in Oxisols under shade and unshaded coffee systems on farmer's fields in Brazil. Agrofor Syst 58:55–64

Cross AF, Schlesinger WH (1995) A literature review and evaluation of the Hedley fractionation: application to the biogeochemical cycle of soil phosphorus in natural ecosystems. Geoderma 64:197–214

Doblas-Miranda E, Sánchez-Piñero F, González-Megías A (2009) Different structuring factors but connected dynamics shape litter and belowground soil macrofaunal food webs. Soil Biol Biochem 41:2543–2550

Frizano J, Johnson AH, Vann DR, Scatena FN (2002) Soil phosphorus fractionation during forest development on landslide scars in the Luquillo Mountains, Puerto Rico. Biotropica 34:17–26

Frizano J, Vann DR, Johnson AH, Johnson CM, Vieira ICG, Zarin DJ (2003) Labile phosphorus in soils of forest fallows and primary forest in the Bragantina region, Brazil. Biotropica 35:2–11

Frossard E, Condrom LM, Oberson A, Sinaj S, Fardeau JC (2000) Processes governing phosphorus availability in temperate soils. J Environ Qual 29:15–23

Garci-Montiel DC, Neill C, Melillo J, Thomas S, Steudler PA, Cerri CC (2000) Soil phosphorus transformations following forest clearing for pasture in the Brazilian Amazon. Soil Sci Soc Am J 64:1792–1804

Giardina CP, Sanford RL, Dockersmith IC (2000) Changes in soil phosphorus and nitrogen during slash-and-burn clearing of a dry tropical forest. Soil Sci Soc Am J 64:399–405

Gijsman AJ, Oberson A, Tiessen H, Friesen DK (1996) Limited applicability of the CENTURY model to highly weathered tropical soils. Agron J 88:894–903

Grace JB (2006) Structural equation modeling and natural systems. Cambridge University Press, New York, p 365

Grace JB, Bollen KA (2008) Representing general theoretical concepts in structural equation models: the role of composite variables. Environ Ecol Stat 15:191–213

Grierson PF, Smithson P, Nziguheba G, Radersma S, Comerford NB (2004) Phosphorus dynamics and mobilization by plants. In: van Noordwik M, Cadisch G, Ong CK (eds) Below-ground interactions in tropical agroecosystems: concepts and models with multiple plant components. CABI International, Wallingford, pp 127–142

Hair JF, Anderson RE (2010) Multivariate data analysis. Prentice-Hall Inc., Upper Saddle River, p 785

Harrison AF (1987) Soil organic phosphorus: a review of world literature. CAB International, Wallingford, p 257

Hedley MJ, Stewart WB, Chauhan BS (1982) Changes in inorganic and organic soil phosphorus fractions induced by cultivation practices and by laboratory incubations. Soil Sci Soc Am J 46:970–976

Hooper D, Coughlan J, Mullen MR (2008) Structural equation modelling: guidelines for determining model fit. Electron J Bus Res Methods 6:53–60

Kenny DA (2012) Measuring model fit. (http://davidakenny.net/cm/fit.htm)

Kitayama K, Majalap-Lee N, Aiba S (2000) Soil phosphorus transformation and phosphorus-use efficiencies of tropical rainforests along altitudinal gradients of Mount Kinabalu, Borneo. Oecologia 123:342–349

Kline RB (2005) Principles and practice of structural equation modeling. The Guilford Press, New York 366p

Lehmann J, Günther D, Mota MS, Almeida MP, Zech W, Kaiser K (2001) Inorganic and organic soil phosphorus and sulfur pools in an Amazonian multistrata agroforestry system. Agrofor Syst 53:113–124

Leite FP (2001) Relações nutricionais e alterações de características químicas de solos da região do Vale do Rio Doce pelo cultivo do eucalipto. Viçosa, Universidade Federal de Viçosa, p 67 (Ph.D. Thesis)

Lilienfein J, Wilcke W, Ayarza MA, Vilela L, Lima SC, Zech W (2000) Chemical fractionation of phosphorus, sulphur, and molybdenum in Brazilian savannah Oxisols under different land use. Geoderma 96:31–46

Linquist BA, Singleton PW, Cassman KG (1997) Inorganic and organic phosphorus dynamics during a build-up and decline of available phosphorus in an Ultisol. Soil Sci 162:254–264

Malaeb ZA, Summers JK, Pugesek BH (2000) Using structural equation modeling to investigate relationships among ecological variables. Environ Ecol Stat 7:93–111

Mardia KV (1974) Applications of some measures of multivariate skewness and kurtosis in testing normality and robustness studies. Indian Stat Inst 36:115–128

Mitchell RJ (1992) Testing evolutionary and ecological hypotheses using path analysis and structural equation modeling. Funct Ecol 6:123–129

Möller A, Kaiser K, Amelung W, Niamskul C, Udomsri S, Puthawong M, Haumaier L, Zech W (2000) Forms of organic C and P extracted from tropical soils as assessed by liquid-state ^{13}C- and ^{31}P-NMR spectroscopy. Aust J Soil Res 38:1017–1035

Mulaik SA (2009) Linear causal modeling with structural equations. CRC Press, Boca Raton, p 428

Negassa W, Leinweber P (2009) How does the Hedley sequential phosphorus fractionation reflect impacts of land use and management on soil phosphorus: a review. J. Plant Nutr Soil 172:305–325

Neufeldt H, Silva JE, Ayarza MA, Zech W (2000) Land-use effects on phosphorus fractions in Cerrado oxisols. Biol Fertil Soils 31:30–37

Newbery DMcC, Alexander IJ, Rother JA (1997) Phosphorus dynamics in a lowland African rain forest: the influence of ectomycorrhizal trees. Ecol Monogr 67:367–409

Novais RF, Smyth TJ (1999) Fósforo em solo e planta em condições tropicais. Viçosa, UFV 399 p

Oberson A, Friesen DK, Rao IM, Bühler S, Frossard E (2001) Phosphorus transformations in an Oxisol under contrasting land use systems: the role of the soil microbial biomass. Plant Soil 237:197–210

Olander LP, Bustamante MM, Asner GP, Telles E, Prado Z, Camargo PB (2005) Surface soil change following selective logging in an eastern Amazon forest. Earth Interact 9:1–19

Prober SM, Wiehl G (2011) Relationships among soil fertility, native plant diversity and exotic plant abundance inform restoration of forb-rich eucalypt woodlands. Divers Distrib 1–13. doi:10.1111/j.1472-4642.2011.00872.x

Reed SC, Townsend AR, Taylor PG, Cleveland CC (2011) Phosphorus cycling in tropical forests growing on highly weathered soils. In: Bünemann EK, Oberson A, Frossard E (eds) Phosphorus in action: biological processes in soil phosphorus cycling. Springer, Berlin, pp 339–369

Sato S, Comerford NB (2006) Organic anions and phosphorus desorption and bioavailability in a humid Brazilian Ultisol. Soil Sci 171:695–705

Sharpley AN, Tiessen H, Cole CV (1987) Soil phosphorus forms extracted by soil tests as a function of pedogenesis. Soil Sci Soc Am J 51:362–365

Smeck NE (1985) Phosphorus dynamics in soils and landscapes. Geoderma 36:185–199

Solomon D, Lehmamn J (2000) Loss of phosphorus from soil in semi-arid northern Tanzania as result of cropping: evidence from sequential extraction and ^{31}P-NMR spectroscopy. Euro J Soil Sci 51:699–708

Solomon D, Lehmamn J, Mamo T, Fritzsche F, Zech W (2002) Phosphorus compounds and dynamics as influenced by land use changes in the sub-humid Ethiopian highlands. Geoderma 105:21–48

Szott LT, Melendez G (2001) Phosphorus availability under annual cropping, alley cropping, and multistrata agroforestry systems. Agrofor Syst 53:125–1132

Tchienkoua M, Zech W (2003) Chemical and spectral characterization of soil phosphorus under three land uses from an Andic Palehumult in West Cameroon. Agric Ecosyst Environ 100:193–200

Tiessen H, Moir JO (1993) Characterisation of available P by sequential extraction. In: Carter MR (ed) Soil sampling and methods of soil analysis. CRC Press, Boca Raton, FL, pp 75–86

Tiessen H, Stewart WB, Cole CV (1984) Pathways of phosphorus transformations in soils of differing pedogenesis. Soil Sci Soc Am J 48:853–858

Tiessen H, Salcedo IH, Sampaio EVSB (1992) Nutrient and soil organic matter dynamics under shifting cultivation in semi-arid northeastern Brazil. Agric Ecosyst Environ 38:139–151

Travis SE, Grace JB (2010) Predicting performance for ecological restoration: a case study using *Spartina alterniflora*. Ecol Appl 20:192–204

Turner BL, Engelbrecht BMJ (2011) Soil organic phosphorus in lowland tropical rain forests. Biogeochemistry 103:297–315

Williams WA, Jones MB, Demment MW (1990) A concise table for path analysis statistics. Agron J 82:1022–1024

Zheng Z, Simard RR, Lafond J, Parent LE (2002) Pathways of soil phosphorus transformations after 8 years of cultivation under contrasting cropping practices. Soil Sci Soc Am J 66:999–1007